The Aeronautical Journal (2025), **129**, pp. 1286–1302
doi:10.1017/aer.2024.120

RESEARCH ARTICLE

Full-state-constrained intelligent adaptive control for nonlinear systems with unmodeled dynamics and mismatched disturbances

Y. Yin[1,2], X. Ning[1,2], Z. Wang[1,3,4,5] and R. Li[6]

[1]National Key Laboratory of Aerospace Flight Dynamics, Northwestern Polytechnical University, Xi'an, China
[2]School of Astronautics, Northwestern Polytechnical University, Xi'an, China
[3]Research Center for Unmanned System Strategy Development, Northwestern Polytechnical University, Xi'an, China
[4]Northwest Institute of Mechanical and Electrical Engineering, Xianyang, China
[5]Unmanned System Research Institute, Northwestern Polytechnical University, Xi'an, China
[6]AECC South Industry Company Limited, Zhuzhou, China
Corresponding author: Z. Wang; Email: wz_nwpu@126.com

Received: 11 March 2024; **Revised:** 23 September 2024; **Accepted:** 8 October 2024

Keywords: adaptive neural network control; full-state constraints; mismatched disturbance; unmodeled dynamics

Abstract

This paper develops a novel full-state-constrained intelligent adaptive control (FIAC) scheme for a class of uncertain nonlinear systems under full state constraints, unmodeled dynamics and external disturbances. The key point of the proposed scheme is to appropriately suppress and compensate for unmodeled dynamics that are coupled with other states of the system under the conditions of various disturbances and full state constraints. Firstly, to guarantee that the time-varying asymmetric full state constraints are obeyed, a simple and valid nonlinear error transformation method has been proposed, which can simplify the constrained control problem of the system states into a bounded control problem of the transformed states. Secondly, considering the coupling relationship between the unmodeled dynamics and other states of the controlled system such as system states and control inputs, a decoupling approach for coupling uncertainties is introduced. Thereafter, owing to the employed dynamic signal and bias radial basis function neural network (BIAS-RBFNN) improved on traditional RBFNN, the adverse effects of unmodeled dynamics on the controlled system can be suppressed appropriately. Furthermore, the matched and mismatched disturbances are reasonably estimated and circumvented by a mathematical inequality and a disturbance observer, respectively. Finally, numerical simulations are provided to demonstrate the effectiveness of the proposed FIAC strategy.

1.0 Introduction

As is known to all, it is unavoidable to encounter various constraints in actual systems. When these constraints are not satisfied, the performance and stability of the system will be affected to various degrees. In recent years, the research on state-constrained control, which mainly includes output-constrained control and full-state-constrained control, has become a hot issue studied by scholars in the field of control [1–6]. Full state constraints not only require system outputs to satisfy constraints but also have constraints on other states of the system. Therefore, in most practical applications, the full state constraints which can avoid excessive overshoot are more general than the output constraints [1]. Currently, the barrier Lyapunov functions (BLFs) have become the main tool to ensure that the full state constraints are obeyed [2, 7–9]. With the aid of BLF and the adaptive backstepping method, a novel adaptive tracking control algorithm for the strict-feedback nonlinear systems with full state constraints and dead zone was studied in [7]. In Ref. [8], based on the tan-type time-varying asymmetric BLF, an adaptive asymptotic tracking control method for the nonlinear systems with parametric uncertainty and time-varying asymmetric full state constraints was developed. Similarly, by introducing the time-varying asymmetric

© The Author(s), 2024. Published by Cambridge University Press on behalf of Royal Aeronautical Society.

https://doi.org/10.1017/aer.2024.120 Published online by Cambridge University Press

BLF in Ref. [9], all state variables were confined to predefined regions. However, considering practical engineering applications, the full-state-constrained control schemes mentioned above do not take into account the complex dynamic coupling uncertainties that may occur in the controlled nonlinear systems, which may lead to the inability to guarantee stability.

It is widely known that disturbances and uncertainties are inevitable in many practical control systems, such as flight control systems, robotics, vehicle systems and mechanical systems and so on [10–14]. However, various disturbances and uncertainties are usually nonlinear, unknown, and coupled with other variables, which makes their mathematical modeling and the design of effective suppression properties difficult. Therefore, the problem of compensation and suppression of disturbances and uncertainties has received extensive attention in the past few decades [14–21]. These come in a variety of forms, including sliding mode control (SMC) [14, 15], active disturbance rejection control (ADRC) [16–18], disturbance observer-based control (DOBC) [14, 19] and adaptive backstepping control (BC) [20, 21]. For a class of robotic systems with matched and mismatched disturbances, a high-order disturbance observer based sliding mode control method was designed in Ref. [14], which can successfully stabilise the robotic systems and suppress the matched and mismatched disturbances effectively. To realise the predictive state and the total uncertainty which represents the effects of the unknown nonlinear dynamics and external disturbances, an extended state observer was developed as a predictor in Ref. [16]. By using the backstepping technique, the authors in Ref. [20] designed an adaptive neural network controller for the uncertain nonlinear systems suffering from input delay and disturbances. In Ref. [21], an adaptive fuzzy backstepping dynamic surface controller was constructed for a class of strict-feedback uncertain nonlinear systems with unknown external disturbances. It is worth noting that the control methods mentioned above are all aimed at handling a single source of disturbances and uncertainties. There are usually multi-source disturbances and uncertainties acting on the actual physical systems, and the characteristic of the complex dynamic coupling in the multi-source uncertainties makes the design of the controller more challenging. Therefore, how to develop a controller to attenuate the effects of dynamic multi-source coupling uncertainties of the controlled system is still an open issue, which motivates this study again.

Motivated by the above discussions, a novel full-state-constrained intelligent adaptive control (FIAC) scheme is proposed for a class of nonlinear systems with unmodeled dynamics and mismatched disturbances in this study. The main contributions can be summarised as follows:

- Different from most of the existing results on the control of uncertain nonlinear systems, this work takes into account the unmodeled dynamics that are coupled with the system states and control inputs and designs a decoupling method based on dynamic signal and improved RBFNN, namely BIAS-RBFNN, to estimate and circumvent the coupling uncertainties.
- To improve the approximation accuracy and anti-disturbance ability of traditional RBFNN, the BIAS-RBFNN is introduced in this paper.
- Compared to the existing state-constrained control schemes with multiple parameters and complex forms in Ref. [22], this work proposed a simple and effective nonlinear error transformation method to transform the constrained control problem of the system states into a bounded control problem of the transformed states, which greatly reduces the difficulty of controller design.
- This paper provides a BIAS-RBFNN-based FIAC canonical form for the nonlinear systems, which can be applied to many other practical systems like robots, quadrotors, space unmanned systems, underwater unmanned systems, and so on.

This paper is organised as follows. In the next section, the full-state-constrained control problem with unmodeled dynamics and disturbances is formulated and some related assumptions and lemmas are introduced. Moreover, we give a detailed description of the novel BIAS-RBFNN. Then, the structure of the proposed full-state-constrained intelligent adaptive control scheme is built, followed by stability

https://doi.org/10.1017/aer.2024.120 Published online by Cambridge University Press

Table 1. *The main variables in this paper*

Item	Nomenclature
$x_1(t), x_2(t)$	System states
$d_1(t), d_2(t)$	Mismatched disturbance and matched disturbance
$f(x_1(t), x_2(t))$	Smooth nonlinear function
$\Delta f(x_1(t), x_2(t))$	Unknown model uncertain item
$\zeta(t)$	Unmodeled dynamics
$\Lambda(x_1(t), x_2(t), u(t), \zeta(t))$	Coupling uncertain term
B	System inertia matrix
$u(t)$	Actual loop controller
$u_c(t)$	Nominal outer loop controller
$x_d(t)$	Desired signal
$\varphi_1(\cdot), \varphi_2(\cdot)$	Unknown non-negative smooth functions
$e_1(t), e_2(t)$	Tracking errors
$s_0(t), s_1(t), s_2(t)$	Transformed states of tracking errors
$x_{2c}(t)$	Virtual control signal
$D(t)$	Total disturbance
Θ	Optimal weight of RBFNN
$\Phi(Z)$	Activation function of RBFNN
$\Phi_b(Z)$	Activation function with local errors
μ_e^s, L_e^s	Variables related to the derivative of transformed states $s_1(t), s_2(t)$
ε_v, ϑ	Adaptive parameters to be designed
$\hat{a}$	Estimate of a
$\hat{a}$	Estimation error of a, and $\tilde{a} = \hat{a} - a$

analysis. Finally, simulations are performed to verify the effectiveness of the proposed control method and a conclusion is presented.

2.0 Problem formulation and preliminaries

2.1 Problem statement

Consider the following nonlinear system subject to unmodeled dynamics, coupling uncertainties and disturbances:

$$\begin{aligned}
\dot{x}_1(t) &= x_2(t) + d_1(t) \\
\dot{x}_2(t) &= f(x_1(t), x_2(t)) + \Delta f(x_1(t), x_2(t)) + \Lambda(x_1(t), x_2(t), u(t), \zeta(t)) + B(u(t) + d_2(t)) \\
\dot{\zeta}(t) &= f_\zeta(\zeta(t), x_1(t), x_2(t), u(t)),
\end{aligned} \tag{1}$$

where $x_1(t), x_2(t)$ denote the states, $u(t)$ is the input signal of the controlled system. $f(x_1(t), x_2(t))$ is the smooth nonlinear function and $\Delta f(x_1(t), x_2(t))$ denotes the model uncertain item. B is a known matrix with proper dimensions and its smallest eigenvalue satisfies $\lambda_{B,min} \geqslant 1$. $d_1(t)$ and $d_2(t)$ denote the mismatched and matched disturbances, respectively. With a reasonable analysis, it is assumed that the coupling uncertain term $\Lambda(x_1(t), x_2(t), u(t), \zeta(t))$ is simultaneously affected by the system states $x_1(t), x_2(t)$, the input signal $u(t)$, and the unmodeled dynamics $\zeta(t)$. What's more, the dynamic characteristics of $\zeta(t)$ can be expressed as $\dot{\zeta}(t) = f_\zeta(\zeta(t), x_1(t), x_2(t), u(t))$. In this paper, the time-varying asymmetric full state constraints are considered, that is, $\underline{b}_1(t) < x_1(t) < \bar{b}_1(t)$ and $\underline{b}_2(t) < x_2(t) < \bar{b}_2(t)$, where all the predefined constraints are bounded. Table 1 shows the main variables used in this work, and more details in this table will be introduced in the following sections.

https://doi.org/10.1017/aer.2024.120 Published online by Cambridge University Press

Our control objective is summarised as follows. Given the nonlinear system Equation (1) with unmodeled dynamics, matched disturbance and mismatched disturbances, the control objective is to propose a full-state-constrained intelligent adaptive controller that can force the system output to track the desired trajectory $x_d(t)$ as far as possible, and all the states satisfy the full state constraints.

2.2 Assumptions and lemmas

To achieve the control objective, the following related assumptions and lemmas are required.

Assumption 1. *The system states $x_1(t)$ and $x_2(t)$ are both accessible. The desired signal $x_d(t)$ is bounded, smooth and twice differentiable.*

Assumption 2. *The coupling uncertainty satisfies the following inequality*

$$\Lambda\left(x_1(t), x_2(t), u(t), \zeta(t)\right) \le \varphi_1\left(x_1(t), x_2(t)\right) + \varphi_2\left(\zeta(t)\right) + p_u u(t) \tag{2}$$

where $\varphi_1(\cdot)$ and $\varphi_2(\cdot)$ are both unknown non-negative smooth functions, $p_u \in (-1, 1)$ is a constant.

Assumption 3. *The unmodeled dynamics are exponentially input-to-state practically stable(exp-ISpS), specifically, there has a Lyapunov function $V_\zeta(\zeta(t))$ so that*

$$\begin{aligned} &\alpha_1\left(\zeta(t)\right) \le V_\zeta\left(\zeta(t)\right) \le \alpha_2\left(\zeta(t)\right) \\ &\frac{\partial V_\zeta\left(\zeta(t)\right)}{\partial \zeta(t)} \kappa\left(\zeta(t), x_1(t), x_2(t), u(t)\right) \le -\gamma_1 V_\zeta\left(\zeta(t)\right) + \rho\left(x_1(t), x_2(t)\right) + \gamma_2, \end{aligned} \tag{3}$$

where $\alpha_1(\cdot), \alpha_2(\cdot)$ belong to class K_∞ functions, $\rho\left(x_1(t), x_2(t)\right) = {x_1}^T(t) x_1(t) + {x_2}^T(t) x_2(t)$, and γ_1, γ_2 are positive constants.

Assumption 4. *For the unknown total disturbance $D(t)$, there exists an unknown positive constant ε_v such that $|D(t)| \le \varepsilon_v$. What's more, the rate of mismatched disturbance $d_1(t)$ is assumed to be bounded, that is $\left\|\dot{d}_1(t)\right\| \le \bar{d}_1$.*

Assumption 5. *The initial values of the system states are all within the predefined constraints, i.e. $\underline{b}_1(0) < x_1(0) < \bar{b}_1(0), \underline{b}_2(0) < x_2(0) < \bar{b}_2(0)$.*

Remark 1. Considering the possible coupling relationship between the unmodeled dynamics $\zeta(t)$ and other states in the nonlinear system, Assumption 2 briefly gives the common constraints for the coupling uncertainties $\Lambda\left(x_1(t), x_2(t), u(t), \zeta(t)\right)$. Assumption 3 provides some standard requirements of the unmodeled dynamics.

Lemma 1. *[23] Given any constant satisfying $\varepsilon > 0$ and any variable $z \in \mathbb{R}$, the following inequality holds*

$$0 \le |z| - z\tanh\left(\frac{z}{\varepsilon}\right) \le \kappa\varepsilon \tag{4}$$

where κ is a constant satisfying $\kappa = \mathrm{e}^{-(\kappa+1)}$, i.e., $\kappa = 0.2785$.

Lemma 2. *[24] For any constant $\varepsilon > 0$ and vector $\xi \in \mathbb{R}^n$, we have*

$$\|\xi\| < \frac{\xi^T \xi}{\sqrt{\xi^T \xi + \varepsilon^2}} + \varepsilon \tag{5}$$

Lemma 3. *[24] For any positive constant $\varepsilon > 0$ take into account the set Ω_ε defined by $\Omega_\varepsilon := \{x \mid \|x\| \le 0.2554\varepsilon\}$. Next, for any $x \notin \Omega_\varepsilon$, the following inequality is satisfied*

$$1 - 16\tanh^2\left(\frac{x}{\varepsilon}\right) \le 0 \tag{6}$$

https://doi.org/10.1017/aer.2024.120 Published online by Cambridge University Press

Lemma 4. *[25] Let $f:\mathbb{R}\to\mathbb{R}$ represents any continuous differentiable function defined on $[0,\infty)$, and $\lim_{t\to\infty} f(t)$ exists and possesses upper bound. If its derived function $\dot{f}(t)$ is uniformly continuous, then $\lim_{t\to\infty}\dot{f}(t)=0$.*

2.3 BIAS-RBFNN

Owing to the capacity of online learning and universal approximation of smooth nonlinear functions, adaptive neural network (ANN) control algorithms have been widely utilised to compensate for the effects caused by unmodeled dynamics or disturbances [26–29]. Among these neural network control algorithms, RBFNN has become the most commonly used one because of its outstanding capacity for function approximation and fast calculation speed. However, to improve the approximation accuracy, the normal RBFNN-based control methods require more hidden nodes, which will increase the computational cost exponentially. In addition, the failure of the approximation may occur when the input of normal RBFNN deviates from the 'approximation domain'. In order to solve the problems mentioned above, we will introduce an adaptive BIAS-RBFNN based control scheme, the conclusion that the anti-disturbance ability of the BIAS-RBFNN based scheme is stronger than the normal RBFNN based scheme has been proved by [30].

According to Ref. [31], for any bounded continuous function $F(Z)$ which is defined on a closed set Ω_Z, the structure of RBFNN can be represented as follows

$$F(Z)=\Theta^T\Phi(Z)+\varepsilon_\Theta(Z),\forall Z\in\Omega_Z \tag{7}$$

where $Z\in\mathbb{R}^n$ is the input vector, Θ denotes the optimal weight. ε_Θ is the optimal approximate error which can be reduced to any tiny value by increasing the number of nodes of the neural network. According to relevant references, the Gaussian functions are often used as the activation functions of RBFNN, which can be described as

$$S_j(Z)=\exp\left[-\frac{(Z-\mu_j)^T(Z-\mu_j)}{\sigma^2}\right],j=1,2,\ldots,m \tag{8}$$

where $\mu_j=\left[\mu_{j1},\mu_{j2},\ldots,\mu_{jn}\right]^T$ represents the position of the hidden node, σ denotes the width of Gaussian functions, m is the number of hidden nodes in each channel.

The activation functions for the adaptive BIAS-RBFNN based control scheme taken in this paper are shown below

$$\Phi_{lj}(Z)=S_j(Z)+b_l \tag{9}$$

where b_l represents the bias of each activation function, which is added to each activation function. According to Ref. [32], $\Phi_{lj}(Z)$ defined in Equation (9) meets the condition of the Tauber-Wiener function, which also has the capability to represent any continuous functions. Considering the length of this paper, we directly give the following lemma:

Lemma 5. *[30] For the target functions with external disturbances, the RBFNNs with bias are more likely to achieve a higher approximation accuracy than the scheme of RBFNNs without bias.*

Based on Lemma 2.3, we can conclude that the BIAS-RBFNN-based control scheme discussed in this section can obtain more accurate function approximation results, and its anti-disturbance ability is stronger.

https://doi.org/10.1017/aer.2024.120 Published online by Cambridge University Press

3.0 Controller design and stability analysis

3.1 Nonlinear error transformation

To satisfy the time-varying full state constraints, a practical approach is to constrain the tracking errors of the system states. In general, most existing works can only ensure that the tracking errors ultimately converge, while ignoring the dynamic performance of the system, which may lead to inevitable oscillations and overshoots. Therefore, this work will propose a simple and effective nonlinear error transformation technique to enable the system states to smoothly track the desired signals without exceeding their constraint range.

By defining the desired output signal $x_d(t)$, the tracking error of $x_1(t)$ and $x_2(t)$ can be expressed as

$$\begin{aligned} e_1(t) &= x_1(t) - x_d(t) \\ e_2(t) &= x_2(t) - x_{2c}(t) \end{aligned} \tag{10}$$

where $x_{2c}(t)$ is the virtual control signal of $e_1(t)$ subsystem.

From the previous analysis, the constraints of the tracking errors can be expressed as

$$\begin{aligned} \underline{e}_1(t) &= \underline{b}_1(t) - x_d(t) \\ \bar{e}_1(t) &= \bar{b}_1(t) - x_d(t) \\ \underline{e}_2(t) &= \underline{b}_2(t) - x_{2c}(t) \\ \bar{e}_2(t) &= \bar{b}_2(t) - x_{2c}(t) \end{aligned} \tag{11}$$

It is clear that if the error constraints $\underline{e}_1(t) < e_1(t) < \bar{e}_1(t)$ and $\underline{e}_2(t) < e_2(t) < \bar{e}_2(t)$ can be well ensured, the system states $x_1(t)$ and $x_2(t)$ can also be guaranteed to never violate the predefined constraints $\left(\underline{b}_1(t), \bar{b}_1(t)\right)$ and $\left(\underline{b}_2(t), \bar{b}_2(t)\right)$, respectively. To guarantee the constraints of the tracking errors, the nonlinear error transformation technique based on a one-one mapping is utilised. Specifically, we define

$$\begin{aligned} s_1(t) &= \tan\left(\frac{\pi}{2} \times \frac{2e_1(t) - \bar{e}_1(t) - \underline{e}_1(t)}{\bar{e}_1(t) - \underline{e}_1(t)}\right) \\ s_2(t) &= \tan\left(\frac{\pi}{2} \times \frac{2e_2(t) - \bar{e}_2(t) - \underline{e}_2(t)}{\bar{e}_2(t) - \underline{e}_2(t)}\right) \end{aligned} \tag{12}$$

Remark 2. The main idea of nonlinear error transformation is that when the original constraint states contact the constraint boundary, the transformed states will tend toward infinity. Generally, some basic functions will approach infinity at their own singular points, which can help us achieve the above results, such as the independent variable of the tangent function approaching $\frac{\pi}{2}$, the antilogarithm of the logarithmic function approaching 0, and so on.

Then, we can get that

$$\begin{aligned} e_1(t) &= \frac{\bar{e}_1(t) - \underline{e}_1(t)}{\pi}\arctan\left(s_1(t)\right) + \frac{\bar{e}_1(t) + \underline{e}_1(t)}{2} \\ e_2(t) &= \frac{\bar{e}_2(t) - \underline{e}_2(t)}{\pi}\arctan\left(s_2(t)\right) + \frac{\bar{e}_2(t) + \underline{e}_2(t)}{2} \end{aligned} \tag{13}$$

By further analysis, we can conclude that

$$\begin{cases} \lim_{s_1 \to -\infty} e_1(t) = \underline{e}_1(t) \\ \lim_{s_1 \to +\infty} e_1(t) = \bar{e}_1(t) \end{cases}, \begin{cases} \lim_{s_2 \to -\infty} e_2(t) = \underline{e}_2(t) \\ \lim_{s_2 \to +\infty} e_2(t) = \bar{e}_2(t) \end{cases} \tag{14}$$

Therefore, we can draw a conclusion that if the transformed states $s_1(t)$ and $s_2(t)$ are bounded, the tracking errors $e_1(t)$ and $e_2(t)$ will consequently be forced to stay within their constraint regions. To achieve this goal, the control problem can be converted to designing a proper adaptive control law to force the transformed states to be bounded.

https://doi.org/10.1017/aer.2024.120 Published online by Cambridge University Press

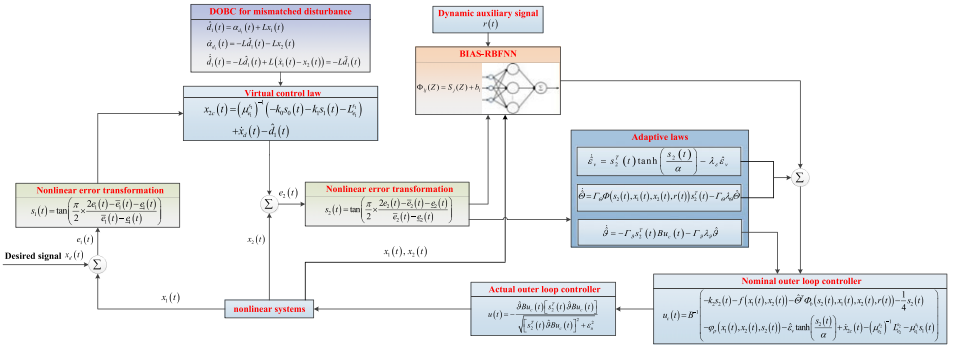


Figure 1. *The structure of the proposed full-state-constrained intelligent adaptive control algorithm.*

3.2 Full-state-constrained intelligent adaptive controller design

In this section, a full-state-constrained BIAS-RBFNN-based intelligent adaptive controller will be constructed and the structure of the proposed control algorithm is demonstrated in Fig. 1.

Taking the derivative of $s_1(t)$ yields

$$\dot{s}_1(t) = \mu_{e_1}^{s_1}(x_2(t) + d_1(t) - \dot{x}_d(t)) + L_{e_1}^{s_1}, \tag{15}$$

where $\mu_{e_1}^{s_1} = \frac{\partial s_1(t)}{\partial e_1(t)}$, $L_{e_1}^{s_1} = \frac{\partial s_1(t)}{\partial \bar{e}_1(t)}\dot{\bar{e}}_1(t) + \frac{\partial s_1(t)}{\partial \underline{e}_1(t)}\dot{\underline{e}}_1(t)$.

By defining $s_0(t) = \int_0^t s_1(u)\ du$, the inner loop virtual signal $x_{2c}(t)$ can be designed as

$$x_{2c}(t) = \left(\mu_{e_1}^{s_1}\right)^{-1}\left(-k_0 s_0(t) - k_1 s_1(t) - L_{e_1}^{s_1}\right) + \dot{x}_d(t) - \hat{d}_1(t) \tag{16}$$

where k_0 and k_1 are positive constant feedback gains, $\hat{d}_1(t)$ denotes the estimated value of mismatched disturbance $d_1(t)$. In this paper, a disturbance observer is used to compensate for the unmatched disturbance $d_1(t)$ and the design process is shown below.

$$\begin{aligned}
\hat{d}_1(t) &= \alpha_{d_1}(t) + Lx_1(t) \\
\dot{\alpha}_{d_1}(t) &= -L\hat{d}_1(t) - Lx_2(t) \\
\dot{\hat{d}}_1(t) &= -L\hat{d}_1(t) + L(\dot{x}_1(t) - x_2(t)) = -L\tilde{d}_1(t)
\end{aligned} \tag{17}$$

where $\tilde{d}_1(t) = \hat{d}_1(t) - d_1(t)$, the gain of the disturbance observer is represented by L, and $\alpha_{d_1}(t)$ is the internal state.

Substituting the virtual signal $x_{2c}(t)$ designed in (16) into $\dot{s}_1(t)$ yields that

$$\dot{s}_1(t) = -k_0 s_0(t) - k_1 s_1(t) - \mu_{e_1}^{s_1}\tilde{d}_1(t) + \mu_{e_1}^{s_1} e_2(t) \tag{18}$$

Taking the time derivative of $s_2(t)$ yields

$$\begin{aligned}
\dot{s}_2(t) &= \mu_{e_2}^{s_2}(\dot{x}_2(t) - \dot{x}_{2c}(t)) + L_{e_2}^{s_2} \\
&= \mu_{e_2}^{s_2}\begin{pmatrix} f(x_1(t), x_2(t)) + \Delta f(x_1(t), x_2(t)) + \Lambda(x_1(t), x_2(t), u(t), \zeta(t)) \\ +B(u(t) + d_2(t)) - \dot{x}_{2c}(t) \end{pmatrix} + L_{e_2}^{s_2},
\end{aligned} \tag{19}$$

where $\mu_{e_2}^{s_2} = \frac{\partial s_2(t)}{\partial e_2(t)}$, $L_{e_2}^{s_2} = \frac{\partial s_2(t)}{\partial \bar{e}_2(t)}\dot{\bar{e}}_2(t) + \frac{\partial s_2(t)}{\partial \underline{e}_2(t)}\dot{\underline{e}}_2(t)$.

Then, introduce the dynamic signal $r(t)$ as shown below

$$\dot{r}(t) = -\gamma_0 r(t) + \rho(x_1(t), x_2(t)), r(0) = r_0 \tag{20}$$

where $\gamma_0 \in (0,\ \gamma_1)$.

https://doi.org/10.1017/aer.2024.120 Published online by Cambridge University Press

According to Assumption 2.2, we can get that

$$s_2^T \Lambda\left(x_1(t), x_2(t), u(t), \zeta(t)\right) \leq \left\|s_2^T(t)\right\|\left(\varphi_1\left(x_1(t), x_2(t)\right) + \varphi_2(\zeta(t)) + p_u u(t)\right) \tag{21}$$

Thanks to Lemma 2.2 and Assumption 3, Equation (21) AUcan be rewritten as

$$\begin{aligned} &\left\|s_2^T(t)\right\| \varphi_1\left(x_1(t), x_2(t)\right) \leq s_2^T(t)\,\bar{\varphi}_1\left(s_2(t), x_1(t), x_2(t)\right) + \varepsilon_1 \\ &\left\|s_2^T(t)\right\| \varphi_2(\zeta(t)) \leq \left\|s_2^T(t)\right\| \varphi_2 \circ \alpha_1^{-1}(2r(t)) + \left\|s_2^T(t)\right\| \varphi_2 \circ \alpha_1^{-1}(2\varepsilon_r) \end{aligned} \tag{22}$$

where $\varepsilon_1 > 0$ is an arbitrary constant,

$$\bar{\varphi}_1\left(s_2(t), x_1(t), x_2(t)\right) = \frac{\varphi_1\left(x_1(t), x_2(t)\right) s_2^T \varphi_1\left(x_1(t), x_2(t)\right)}{\sqrt{\left[s_2^T \varphi_1\left(x_1(t), x_2(t)\right)\right]^2 + \varepsilon_1^2}} \tag{23}$$

Further, using Young's inequality, we can get that

$$\left\|s_2^T(t)\right\| \varphi_2(\zeta(t)) \leq s_2^T \bar{\varphi}_2\left(s_2(t), x_1(t), x_2(t), r(t)\right) + \varepsilon_2 + \frac{1}{4} s_2^T(t)\, s_2(t) + \varepsilon_3 \tag{24}$$

where $\varepsilon_2 > 0$ is an arbitrary constant,

$$\begin{aligned} &\bar{\varphi}_2\left(s_2(t), x_1(t), x_2(t), r(t)\right) = \frac{\varphi_2 \circ \alpha_1^{-1}(2r(t))\, s_2^T(t)\, \varphi_2 \circ \alpha_1^{-1}(2r(t))}{\sqrt{\left[s_2^T(t)\, \varphi_2 \circ \alpha_1^{-1}(2r(t))\right]^2 + \varepsilon_2^2}} \\ &\varepsilon_3 = \left[\varphi_2 \circ \alpha_1^{-1}(2\varepsilon_r)\right]^2 \end{aligned} \tag{25}$$

For the set-valued mapping of the outer-loop tracking error, BIAS-RBFNN is introduced to approximate the unknown nonlinear term

$$\begin{aligned} &\Theta^T \Phi_b\left(s_2(t), x_1(t), x_2(t), r(t)\right) + \varepsilon_\Theta = \bar{\varphi}_1\left(s_2(t), x_1(t), x_2(t)\right) + \bar{\varphi}_2\left(s_2(t), x_1(t), x_2(t), r(t)\right) \\ &+ \Delta f\left(x_1(t), x_2(t)\right) x_2(t) + s_2(t)^{-1} s_1(t)\left(e_2(t) - s_2(t)\right) \end{aligned} \tag{26}$$

where ε_Θ is the RBFNN estimation error and $\Phi_b\left(s_2(t), x_1(t), x_2(t), r(t)\right)$ is the activation function with local errors.

In order to compensate and suppress the influence of the matched disturbance $d_2(t)$ and neural network estimation error ε_Θ on the controlled system. Firstly, the total disturbance $D(t)$ can be constructed in the following form:

$$D(t) = B d_2(t) + \varepsilon_\Theta \tag{27}$$

Based on Assumption 4, the following inequality holds

$$|D(t)| = |B d_2(t) + \varepsilon_\Theta| \leq \varepsilon_v \tag{28}$$

According to Lemma 1, it's easy to get that

$$s_2^T(t)\, D(t) \leq |s_2(t)|\, \varepsilon_v \leq \varepsilon_v s_2^T(t) \tanh\left(\frac{s_2(t)}{\alpha}\right) + \kappa \alpha \varepsilon_v \tag{29}$$

In addition, the following inequality can be established by designing the control signal $u(t)$ to satisfy $s_2^T(t)\, u(t) \leq 0$, hence we have

$$\begin{aligned} &s_2^T(t)\, u(t) + \left\|p_u s_2^T(t)\, u(t)\right\| \\ &\leq s_2^T(t)\, u(t) - \|p_u\|\, s_2^T(t)\, u(t) \\ &\leq (1 - \|p_u\|)\, s_2^T(t)\, u(t) \end{aligned} \tag{30}$$

Based on the above analysis, the nominal outer loop controller can be designed as

$$u_c(t) = B^{-1} \begin{pmatrix} -k_2 s_2(t) - f\left(x_1(t), x_2(t)\right) - \hat{\Theta}^T \Phi_b\left(s_2(t), x_1(t), x_2(t), r(t)\right) - \dfrac{1}{4} s_2(t) \\ -\varphi_\rho\left(x_1(t), x_2(t), s_2(t)\right) - \hat{\varepsilon}_v \tanh\left(\dfrac{s_2(t)}{\alpha}\right) + \dot{x}_{2c}(t) - \left(\mu_{e_2}^{s_2}\right)^{-1} L_{e_2}^{s_2} - \mu_{e_1}^{s_1} s_1(t) \end{pmatrix} \tag{31}$$

https://doi.org/10.1017/aer.2024.120 Published online by Cambridge University Press

The meaning of $\varphi_\rho\left(x_1\left(t\right), x_2\left(t\right), s_2\left(t\right)\right)$ will be explained in the following section. Further, by defining $\vartheta = 1/\inf_{t\geqslant 0}\left[B - I\cdot\left\|p_u\right\|\right]$, the actual loop controller can be designed as

$$u\left(t\right) = -\frac{\hat{\vartheta}Bu_c\left(t\right)\left[s_2^T\left(t\right)\hat{\vartheta}Bu_c\left(t\right)\right]}{\sqrt{\left[s_2^T\left(t\right)\hat{\vartheta}Bu_c\left(t\right)\right]^2 + \varepsilon_u^2}} \tag{32}$$

where $\hat{\varepsilon}_v$, $\hat{\Theta}$, $\hat{\vartheta}$ are the estimated values of ε_v, Θ, ϑ, respectively.

Then the adaptive law of $\hat{\varepsilon}_v$, $\hat{\Theta}$, $\hat{\vartheta}$ are proposed as

$$\begin{aligned}
\dot{\hat{\varepsilon}}_v &= s_2^T\left(t\right)\tanh\left(\frac{s_2\left(t\right)}{\alpha}\right) - \lambda_\varepsilon\hat{\varepsilon}_v\\
\dot{\hat{\Theta}} &= \Gamma_\Theta\Phi\left(s_2\left(t\right), x_1\left(t\right), x_2\left(t\right), r\left(t\right)\right)s_2^T\left(t\right) - \Gamma_\Theta\lambda_\Theta\hat{\Theta}\\
\dot{\hat{\vartheta}} &= -\Gamma_\vartheta s_2^T\left(t\right)Bu_c\left(t\right) - \Gamma_\vartheta\lambda_\vartheta\hat{\vartheta}
\end{aligned} \tag{33}$$

where Γ_Θ, Γ_ϑ, λ_ε, λ_Θ, λ_ϑ are all positive design parameters.

To illustrate the effectiveness and stability of the proposed controller designed by the FIAC scheme for a class of uncertain nonlinear systems with unmodeled dynamics, coupling uncertainties, and mismatched disturbances, the stability analysis is given in the following subsection.

3.3 Stability analysis

Based on the above analysis, the differential equations of the controlled nonlinear system can be rewritten as

$$\begin{aligned}
\dot{s}_0\left(t\right) &= s_1\left(t\right)\\
\dot{s}_1\left(t\right) &= -k_0 s_0\left(t\right) - k_1 s_1\left(t\right) - \mu_{e_1}^{s_1}\tilde{d}_1\left(t\right) + \mu_{e_1}^{s_1}e_2\left(t\right)\\
\dot{s}_2\left(t\right) &= \mu_{e_2}^{s_2}\begin{pmatrix} f\left(x_1\left(t\right), x_2\left(t\right)\right) + \Delta f\left(x_1\left(t\right), x_2\left(t\right)\right) + \Lambda\left(x_1\left(t\right), x_2\left(t\right), u\left(t\right), \zeta\left(t\right)\right)\\ +B\left(u\left(t\right) + d_2\left(t\right)\right) - \dot{x}_{2c}\left(t\right)\end{pmatrix} + L_{e_2}^{s_2}\\
\dot{\zeta}\left(t\right) &= f_\zeta\left(\zeta\left(t\right), x_1\left(t\right), x_2\left(t\right), u\left(t\right)\right)
\end{aligned} \tag{34}$$

The purpose of this paper is to design a suitable controller to ensure the stability of the differential equations in Equation (34). The stability of the closed-loop nonlinear system with the proposed control method can be revealed by the following theorem.

Theorem 1. *Consider the nonlinear system shown in Equation (1), which is affected by unmodeled dynamics, coupled uncertainties, and various external disturbances. Assume that Assumption 1 ∼ 5 are satisfied. By using the nonlinear error transformation method Equation (12), the control laws Equations (31), (32), and the adaptive laws Equation (33), all signals have upper bounds and the tracking errors will converge to the compact sets. And all states will not violate their constraint boundaries.*

Proof. *According to Ref. [33], the dynamic signal r (t) has the following properties*

$$\begin{aligned}
&r\left(t\right)\geqslant 0, \forall t\geqslant 0\\
&V_\zeta\left(\zeta\left(t\right)\right)\leq r\left(t\right) + \varepsilon_r
\end{aligned} \tag{35}$$

where $\varepsilon_r = V_\zeta\left(\zeta\left(0\right)\right) + \frac{\gamma_2}{\gamma_1}$. □

By defining $\tilde{\Theta} = \hat{\Theta} - \Theta$, $\tilde{\vartheta} = \hat{\vartheta} - \vartheta$, $\tilde{\varepsilon}_v = \hat{\varepsilon}_v - \varepsilon_v$, the Lyapunov function can be selected as

$$\begin{aligned}
V &= V_1 + V_2, V_1 = \frac{1}{2}s_0^T\left(t\right)s_0\left(t\right) + \frac{1}{2}s_1^T\left(t\right)s_1\left(t\right) + \frac{1}{2}\tilde{d}_1^T\left(t\right)\tilde{d}_1\left(t\right)\\
V_2 &= \frac{1}{2}\left(\mu_{e_2}^{s_2}\right)^{-1}s_2^T\left(t\right)s_2\left(t\right) + \frac{1}{2}Tr\left(\tilde{\Theta}^T\Gamma_\Theta^{-1}\tilde{\Theta}\right) + \frac{1}{2\vartheta\Gamma_\vartheta}\tilde{\vartheta}^2 + \frac{1}{2}\tilde{\varepsilon}_v^T\tilde{\varepsilon}_v + \frac{r}{\Gamma_r}
\end{aligned} \tag{36}$$

where $\Gamma_r > 0$ is a positive constant.

https://doi.org/10.1017/aer.2024.120 Published online by Cambridge University Press

Combining the differential equations in Equation (34), the derivative of V_1 can be expressed as

$$\dot{V}_1 = s_0^T(t)\, s_1(t) + s_1^T(t)\left(-k_0 s_0(t) - k_1 s_1(t) - \mu_{e_1}^{s_1}\tilde{d}_1(t) + \mu_{e_1}^{s_1} e_2(t)\right) + \tilde{d}_1^T(t)\,\dot{\tilde{d}}_1(t) \tag{37}$$

From the designed disturbance observer Equation (17), it's easy to conclude that

$$\dot{\tilde{d}}_1(t) = -L\tilde{d}_1(t) - \dot{d}_1(t) \tag{38}$$

Then, by defining $\bar{s}_1 = \left[s_0^T(t),\ s_1^T(t)\right]^T$ and using the following inequalities

$$\begin{aligned} -\mu_{e_1}^{s_1} s_1^T(t)\,\tilde{d}_1(t) &\le \frac{\mu_{e_1}^{s_1}}{2} s_1^T(t)\, s_1(t) + \frac{\mu_{e_1}^{s_1}}{2}\tilde{d}_1^T(t)\,\tilde{d}_1(t) \\ -\tilde{d}_1^T(t)\,\dot{d}_1(t) &\le \frac{1}{2}\tilde{d}_1^T(t)\,\tilde{d}_1(t) + \frac{1}{2}\dot{d}_1^T(t)\,\dot{d}_1(t) \end{aligned} \tag{39}$$

the derivative of V_1 in Equation (37) can be developed as

$$\begin{aligned} \dot{V}_1 &\le -\bar{s}_1^T(t)\, Q\bar{s}_1(t) - \mu_{e_1}^{s_1} s_1^T(t)\, e_2(t) - \tilde{d}_1^T(t)\left(L\tilde{d}_1(t) + \dot{d}_1(t)\right) + \frac{\mu_{e_1}^{s_1}}{2}\tilde{d}_1^T(t)\,\tilde{d}_1(t) \\ &\le -\bar{s}_1^T(t)\, Q\bar{s}_1(t) - \mu_{e_1}^{s_1} s_1^T(t)\, e_2(t) + \left(\frac{\mu_{e_1}^{s_1}+1}{2} - L\right)\tilde{d}_1^T(t)\,\tilde{d}_1(t) + \frac{1}{2}\dot{d}_1^T(t) + \dot{d}_1(t) \end{aligned} \tag{40}$$

Where,

$$Q = \begin{bmatrix} 0 & -I_n \\ k_0 I_n & (-\frac{\mu_{e_1}^{s_1}}{2} + k_1) I_n \end{bmatrix} \tag{41}$$

Similarly, combining the dynamic characteristics of the dynamic signal $r(t)$ defined by (20), the derivative of V_2 is

$$\dot{V}_2 = \left(\mu_{e_2}^{s_2}\right)^{-1} s_2^T(t)\,\dot{s}_2(t) + Tr\left(\tilde{\Theta}^T \Gamma_\Theta^{-1}\dot{\hat{\Theta}}\right) + \frac{1}{\vartheta\,\Gamma_\vartheta}\tilde{\vartheta}\,\dot{\hat{\vartheta}} + \tilde{\varepsilon}_v^T\dot{\hat{\varepsilon}}_v - \frac{\gamma_0}{\Gamma_r} r(t) + \frac{\rho\left(x_1(t), x_2(t)\right)}{\Gamma_r} \tag{42}$$

Thanks to the differential Equation (34), we can easily obtain that

$$\left(\mu_{e_2}^{s_2}\right)^{-1} s_2^T(t)\,\dot{s}_2(t) = s_2^T(t)\begin{pmatrix} f\left(x_1(t), x_2(t)\right) + \Delta f\left(x_1(t), x_2(t)\right) + \Lambda\left(x_1(t), x_2(t), u(t), \zeta(t)\right) \\ +B\left(u(t) + d_2(t)\right) - \dot{x}_{2c}(t) + \left(\mu_{e_2}^{s_2}\right)^{-1} L_{e_2}^{s_2} \end{pmatrix} \tag{43}$$

Combined with Equations (21)–(25) and (30), one has

$$\begin{aligned} s_2^T(t)\,\Lambda\left(x_1(t), x_2(t), u(t), \zeta(t)\right) &\le e_2^T(t)\,\bar{\varphi}_1\left(s_2(t), x_1(t), x_2(t)\right) + s_2^T(t)\,\bar{\varphi}_2\left(s_2(t), x_1(t), x_2(t), r(t)\right) \\ &+ \frac{1}{4} s_2^T(t)\, s_2(t) - \|p_u\|\, s_2^T(t)\, u(t) + \sum_{i=1}^{3}\varepsilon_i. \end{aligned} \tag{44}$$

With the aid of Equation (26), it's clear that

$$\begin{aligned} &s_2^T(t)\,\Lambda\left(x_1(t), x_2(t), u(t), \zeta(t)\right) + s_2^T(t)\,\Delta f\left(x_1(t), x_2(t)\right) \\ &\le s_2^T(t)\,\Theta^T\Phi_b\left(s_2(t), x_1(t), x_2(t), r(t)\right) + s_2^T(t)\,\varepsilon_\Theta + \frac{1}{4} s_2^T(t)\, s_2(t) - \|p_u\|\, s_2^T(t)\, u(t) + \sum_{i=1}^{3}\varepsilon_i. \end{aligned} \tag{45}$$

https://doi.org/10.1017/aer.2024.120 Published online by Cambridge University Press

Then, combined with Equation (29), the following inequality can be constructed

$$\left(\mu_{e_2}^{s_2}\right)^{-1} s_2^T(t)\,\dot{s}_2(t) \le s_2^T(t)\begin{pmatrix} f(x_1(t),x_2(t)) + \Theta^T\Phi_b(s_2(t),x_1(t),x_2(t),r(t)) + \frac{1}{4}s_2(t) \\ -\|p_u\|\,u(t) + Bu(t) + \varepsilon_v \tanh\left(\frac{s_2(t)}{\alpha}\right) - \dot{x}_{2c}(t) + \left(\mu_{e_2}^{s_2}\right)^{-1} L_{e_2}^{s_2} \end{pmatrix} + \sum_{i=1}^{3}\varepsilon_i + \kappa\alpha\varepsilon_v \tag{46}$$

Substituting $u_c(t)$ into Equation (46) yields that

$$\left(\mu_{e_2}^{s_2}\right)^{-1} s_2^T(t)\,\dot{s}_2(t) \le s_2^T(t)\begin{pmatrix} -k_2 s_2(t) - \varphi_\rho(x_1(t),x_2(t),s_2(t)) + (B - I\|p_u\|)\,u(t) - Bu_c(t) \\ -\tilde{\Theta}^T\Phi_b(s_2(t),x_1(t),x_2(t),r(t)) - \tilde{\varepsilon}_v \tanh\left(\frac{s_2(t)}{\alpha}\right) - \mu_{e_1}^{s_1} s_1(t) \end{pmatrix} + \sum_{i=1}^{3}\varepsilon_i + \kappa\alpha\varepsilon_v \tag{47}$$

Then, referring to Lemma 2.2, we can get that

$$\begin{aligned} & s_2^T(t)(B - I\|p_u\|)\,u(t) - s_2^T(t)\,Bu_c(t) \\ &= -\frac{(B - I\|p_u\|)\left[s_2^T(t)\,\hat{\vartheta}Bu_c(t)\right]^2}{\sqrt{\left[s_2^T(t)\,\hat{\vartheta}Bu_c(t)\right]^2 + \varepsilon_u^2}} - s_2^T(t)\,Bu_c(t) \\ &\le -\frac{1}{\vartheta}\frac{\left[s_2^T(t)\,\hat{\vartheta}Bu_c(t)\right]^2}{\sqrt{\left[s_2^T(t)\,\hat{\vartheta}Bu_c(t)\right]^2 + \varepsilon_u^2}} - s_2^T(t)\,Bu_c(t) \\ &\le \tfrac{1}{\vartheta}\left(-\left\|s_2^T(t)\,\hat{\vartheta}Bu_c(t)\right\| + \varepsilon_u\right) - s_2^T(t)\,Bu_c(t) \\ &\le \frac{1}{\vartheta}\left(\tilde{\vartheta}s_2^T(t)\,Bu_c(t) + \varepsilon_u\right) \end{aligned} \tag{48}$$

For any vector $\xi \in \mathbb{R}^n$, we define

$$\mathrm{Tanh}(\xi(t)) = [\tanh\xi_1(t), \tanh\xi_2(t), \cdots, \tanh\xi_n(t)]^T. \tag{49}$$

Hence, the following formula is established

$$\begin{aligned} \frac{\rho(x_1(t),x_2(t))}{\Gamma_r} &= \frac{\rho(x_1(t),x_2(t))}{\Gamma_r}\left(1 - 16\mathrm{Tanh}^T\left(\frac{s_2^T(t)}{\varepsilon_\rho}\right)\mathrm{Tanh}\left(\frac{s_2^T(t)}{\varepsilon_\rho}\right)\right) \\ &+ s_2^T(t)\,\varphi_\rho(x_1(t),x_2(t),s_2(t)) \end{aligned} \tag{50}$$

where

$$\varphi_\rho(x_1(t),x_2(t),s_2(t)) = \frac{16 s_2(t)\,\rho(x_1(t),x_2(t))}{\Gamma_r s_2^T(t)\,s_2(t)}\mathrm{Tanh}^T\left(\frac{s_2^T(t)}{\varepsilon_\rho}\right)\mathrm{Tanh}\left(\frac{s_2^T(t)}{\varepsilon_\rho}\right) \tag{51}$$

noting that $\varphi_\rho(x_1(t),x_2(t),s_2(t))$ is a non-singular function vector for $s_2(t)$.

https://doi.org/10.1017/aer.2024.120 Published online by Cambridge University Press

Substituting formulas (47), (48), (50) and (51) into formula (42), and combining Equation (40) and Assumption 4, we can derive the result of the differentiation of V as follows

$$\begin{aligned}
&\dot{V} = \dot{V}_1 + \dot{V}_2 \\
&\leq -\bar{s}_1^T(t) Q \bar{s}_1(t) - \left(L - \frac{\mu_{e_1}^{s_1} + 1}{2}\right) \tilde{d}_1^T(t) \tilde{d}_1(t) + \frac{1}{2}\bar{d}_1^2 - k_2 s_2^T(t) s_2(t) \\
&+ \frac{\rho(x_1(t), x_2(t))}{\Gamma_r} \left(1 - 16\mathrm{Tanh}^T\left(\frac{s_2^T(t)}{\varepsilon_\rho}\right)\mathrm{Tanh}\left(\frac{s_2^T(t)}{\varepsilon_\rho}\right)\right) + \frac{\tilde{\vartheta}}{\vartheta} s_2^T(t) B u_c(t). \\
&+ \frac{\varepsilon_u}{\vartheta} - s_2^T(t) \tilde{\Theta}^T \Phi_b(s_2(t), x_1(t), x_2(t), r(t)) - s_2^T(t) \tilde{\varepsilon}_v \tanh\left(\frac{s_2(t)}{\alpha}\right) \\
&+ Tr\left(\tilde{\Theta}^T \Gamma_\Theta^{-1} \dot{\hat{\Theta}}\right) + \frac{1}{\vartheta \Gamma_\vartheta} \tilde{\vartheta} \dot{\hat{\vartheta}} + \tilde{\varepsilon}_v^T \dot{\hat{\varepsilon}}_v - \frac{\gamma_0}{\Gamma_r} r(t) + \sum_{i=1}^{3} \varepsilon_i + \kappa \alpha \varepsilon_v
\end{aligned} \tag{52}$$

By using the adaptive laws Equation (33) and considering the following inequalities

$$\begin{aligned}
&-Tr\left(\tilde{\Theta}^T \hat{\Theta}\right) \leq -\frac{1}{2} Tr\left(\tilde{\Theta}^T \tilde{\Theta}\right) + \frac{1}{2} Tr\left(\Theta^T \Theta\right) \\
&-\tilde{\varepsilon}_v^T \hat{\varepsilon}_v \leq -\frac{1}{2}\tilde{\varepsilon}_v^2 + \frac{1}{2}\varepsilon_v^2 \\
&-\tilde{\vartheta}^T \hat{\vartheta} \leq -\frac{1}{2}\tilde{\vartheta}^2 + \frac{1}{2}\vartheta^2
\end{aligned} \tag{53}$$

Therefore, we can further obtain the following result

$$\begin{aligned}
\dot{V} \leq &-\bar{s}_1^T(t) Q \bar{s}_1(t) - \left(L - \frac{\mu_{e_1}^{s_1} + 1}{2}\right) \tilde{d}_1^T(t) \tilde{d}_1(t) - k_2 s_2^T(t) s_2(t) - \frac{\lambda_\vartheta}{2\vartheta} \tilde{\vartheta}^2 \\
&- \frac{\lambda_\Theta}{2} Tr\left(\tilde{\Theta}^T \tilde{\Theta}\right) - \frac{\lambda_\varepsilon}{2}\tilde{\varepsilon}_v^2 + \frac{1}{2}\bar{d}_1^2 + \frac{\rho(x_1(t), x_2(t))}{\Gamma_r} \left(1 - 16\mathrm{Tanh}^T\left(\frac{s_2^T(t)}{\varepsilon_\rho}\right)\mathrm{Tanh}\left(\frac{s_2^T(t)}{\varepsilon_\rho}\right)\right) \\
&+ \frac{\lambda_\vartheta}{2}\vartheta + \frac{\lambda_\Theta}{2} Tr\left(\Theta^T \Theta\right) + \frac{\lambda_\varepsilon}{2}\varepsilon_v^2 + \frac{\varepsilon_u}{\vartheta} - \frac{\gamma_0}{\Gamma_r} r(t) + \sum_{i=1}^{3} \varepsilon_i + \kappa \alpha \varepsilon_v
\end{aligned} \tag{54}$$

Ultimately, we can get the following conclusions

$$\dot{V} \leq -\gamma V + k_f + \frac{\rho(x_1(t), {}_2(t))}{\Gamma_r} \left(1 - 16\mathrm{Tanh}^T\left(\frac{s_2^T(t)}{\varepsilon_\rho}\right)\mathrm{Tanh}\left(\frac{s_2^T(t)}{\varepsilon_\rho}\right)\right) \tag{55}$$

where

$$\begin{aligned}
&\gamma = \min\left\{2\lambda_{\min}(Q),\ 2L - \left(\mu_{e_1}^{s_1} + 1\right),\ 2\mu_{e_2}^{s_2} k_2,\ \lambda_\varepsilon,\ \lambda_{\min}(\Gamma_\Theta)\lambda_\Theta,\ \Gamma_\vartheta \lambda_\vartheta\right\} \\
&k_f = \frac{\lambda_\Theta}{2} Tr\left(\Theta^T \Theta\right) + \frac{\lambda_\varepsilon}{2}\varepsilon_v^2 + \frac{\lambda_\vartheta}{2}\vartheta + \frac{\bar{d}_1^2}{2} + \frac{\varepsilon_u}{\vartheta} + \sum_{i=1}^{3} \varepsilon_i + \kappa \alpha \varepsilon_v
\end{aligned} \tag{56}$$

Define the following compact set

$$\begin{aligned}
&\Omega_f = \{x \in \mathbb{R}^n \,|\, V(x) \leq \gamma_2/\gamma_1\} \\
&\Omega_\rho = \{x \,|\, \|x\| \leq 0.2554\varepsilon\}
\end{aligned} \tag{57}$$

Based on Lemma 3, it is easy to know that if $s_2(t) \in \Omega_f \cap \Omega_\rho$, the solution of the closed-loop control system $\left[s_0(t), s_1(t), s_2(t), \tilde{\varepsilon}_v(t), \tilde{\Theta}(t), \tilde{\vartheta}(t)\right]$ are naturally bounded. If $s_2(t) \notin \Omega_f \cap \Omega_\rho$, $\dot{V} < 0$ can be proved and $V(t)$ gradually decreases, and the solution will eventually converge to the set $\Omega_f \cap \Omega_\rho$. Furthermore, according to Lemma 4, we know that when $t \to \infty$, $e_1(t) \to 0$, that is, the system tracking error gradually converges to zero. The proof is completed.

https://doi.org/10.1017/aer.2024.120 Published online by Cambridge University Press

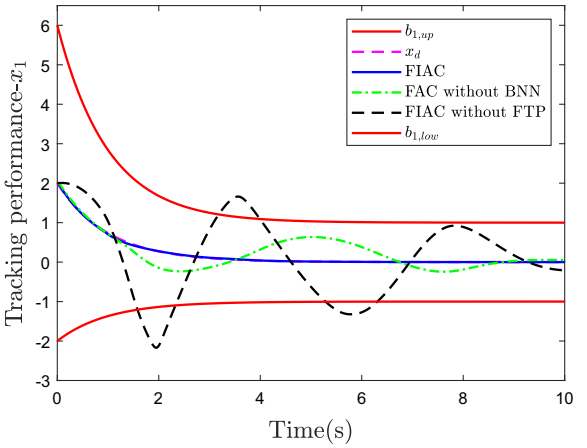


Figure 2. *The tracking performance of x_1 (t) under different control schemes.*

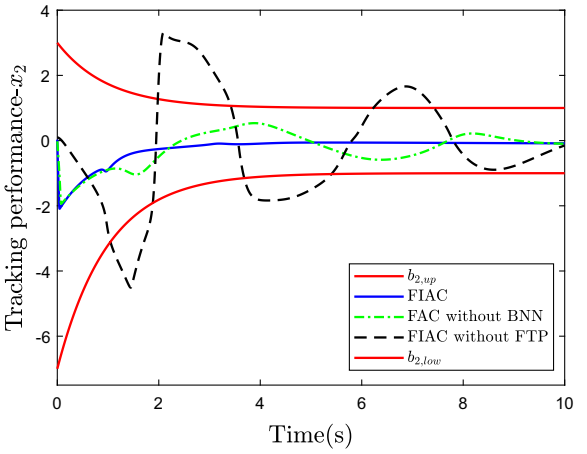


Figure 3. *The tracking performance of x_2 (t) under different control schemes.*

4.0 Simulation study

In this section, numerical simulations are conducted to demonstrate the validity of the proposed FIAC method. The simulations will be carried out in the following two aspects: a comparison of the proposed method with other methods and a comparison of the proposed method under different cases.

Based on the nonlinear system given by Equation (1), the specific parameters are given as

$$\begin{aligned} f\left(x_1\left(t\right), x_2\left(t\right)\right) &= 0.2\sin\left(x_1\left(t\right) + x_2\left(t\right)\right),\ B = 2 \\ \Delta f\left(x_1\left(t\right), x_2\left(t\right)\right) &= 0.1\sin\left(0.2x_1\left(t\right) + 0.1x_2\left(t\right)\right) \end{aligned} \tag{58}$$

The mismatched disturbance and matched disturbance are set as

$$d_1\left(t\right) = 0.1\sin\left(0.1\,t\right),\ \ d_2\left(t\right) = 0.2\sin\left(0.2\,t\right) \tag{59}$$

We choose the unmodeled dynamics as

$$\dot{\zeta}\left(t\right) = -12\zeta\left(t\right) + x_1(t)^T x_1\left(t\right) + x_2(t)^T x_2\left(t\right),\ \ \zeta\left(0\right) = 1 \tag{60}$$

https://doi.org/10.1017/aer.2024.120 Published online by Cambridge University Press

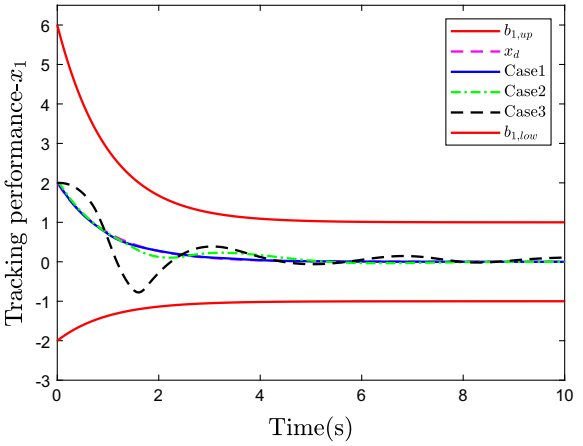


Figure 4. *The tracking performance of $x_1(t)$ of the proposed FIAC scheme under different cases.*

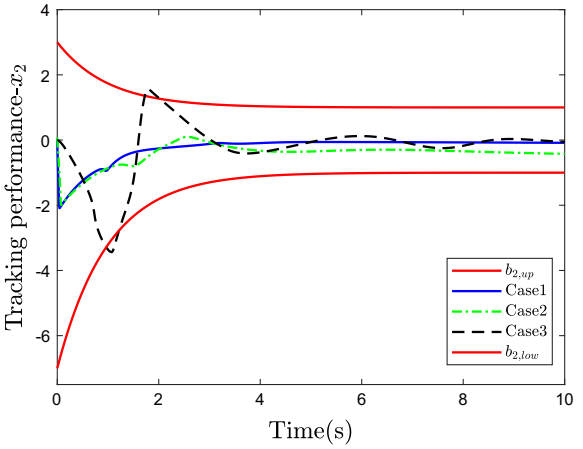


Figure 5. *The tracking performance of $x_2(t)$ of the proposed FIAC scheme under different cases.*

The coupling uncertainty is affected by the system states, the input signal, and the unmodeled dynamics, which is supposed to be

$$\Lambda\left(x_1(t), x_2(t), u(t), \zeta(t)\right) = -2\sin(t)\, x_1(t) + \zeta\left(x_1(t) + x_2(t)\right) - \sin\left(\zeta(t)\right) u(t) \tag{61}$$

What's more, the dynamic auxiliary signal $r(t)$ is designed as

$$\dot{r}(t) = -3r(t) + x_1(t)^T x_1(t) + x_2(t)^T x_2(t), \quad r(0) = 0.5 \tag{62}$$

The time-varying asymmetric constraints of the states are set as

$$\begin{aligned} \underline{b}_1(t) &= -e^{-t} - 1, \bar{b}_1(t) = 5e^{-t} + 1 \\ \underline{b}_2(t) &= -6e^{-t} - 1, \bar{b}_2(t) = 2e^{-t} + 1 \end{aligned} \tag{63}$$

The input of the BIAS-RBFNN is selected as $Z(t) = [x_1(t), x_2(t), s_2(t), r(t)]^T$ and the position of the hidden nodes of each input channel is $[-1,\ 0,\ 1]$, thus the total number of hidden nodes is $3^4 = 81$.

In this simulation, the initial conditions are set as follows: $x_1(0) = 2,\ x_2(0) = 0.1,\ \hat{\varepsilon}_v(0) = 0,\ \hat{\Theta}(0) = [0,\ 0,\ \ldots,\ 0]^T_{1\times 81},\ \hat{\vartheta}(0) = 3$. The control gains are designed as $k_0 = 10,\ k_1 = 4,\ k_2 = 10$. The adaptive parameters are given as $\lambda_\varepsilon = 0.3,\ \lambda_\Theta = 0.1,\ \lambda_\vartheta = 0.2$ and the gains of the adaptive laws

https://doi.org/10.1017/aer.2024.120 Published online by Cambridge University Press

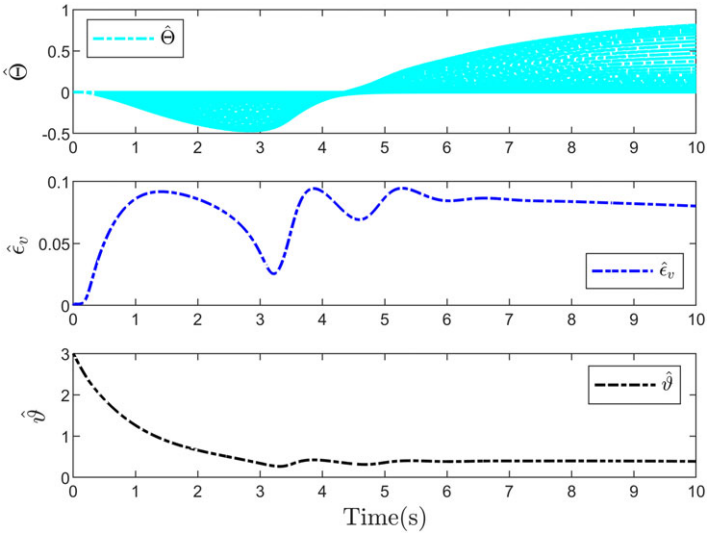


Figure 6. *The trajectories of the adaptive parameters of the proposed FIAC scheme.*

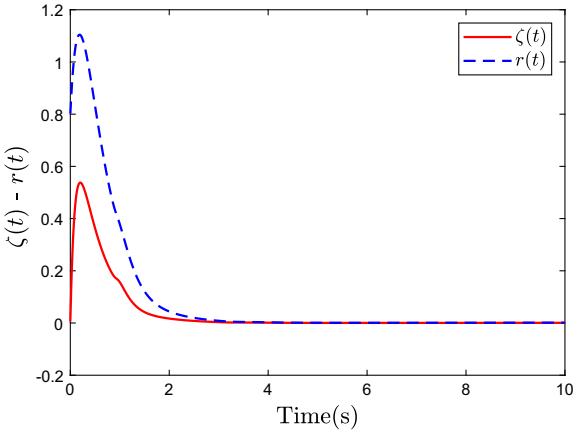


Figure 7. *The trajectories of the auxiliary signal r (t) and the unmodeled dynamics ζ (t).*

are set as $\Gamma_\Theta = 10$, $\Gamma_\vartheta = 1.2$. The constants in the simulation are selected as $\varepsilon_u = 2$, $\varepsilon_\rho = 0.1$, $\alpha = 0.1$, $\Gamma_r = 100$. The gain of the disturbance observer is set as $L = 10$. The time-varying desired signal is generated by $x_d\,(t) = 2e^{-t}$.

The simulation results are provided in Figs. 2–7. To verify the advantages of the proposed FIAC method, the full-state-constrained adaptive control (FAC) method without BIAS-RBFNN (BNN) and the FIAC method without fault-tolerant processing (FTP) are also taken into account for comparison, which is shown in Figs. 2 and 3. It can be seen from Figs. 2 and 3 that the proposed FIAC method can achieve excellent tracking performance and guarantee to never violate the predefined time-varying asymmetric full state constraints in simultaneous presence of the unmodeled dynamics and disturbances, which indicates the control objective has been realised successfully. It is obvious that although the tracking trajectories of the FAC method without BNN and the FIAC method without FTP converge gradually, the dynamic performance of the system is ignored, resulting in nonnegligible oscillation and overshoot, as well as the system states exceeding the constraint boundary. The varying trajectories of the adaptive parameters of the proposed FIAC method are shown in Fig. 6, which demonstrates the boundness of

https://doi.org/10.1017/aer.2024.120 Published online by Cambridge University Press

Table 2. *Three different cases of the simulation experiment*

Uncertainties	Case1	Case2	Case3
$d_1(t)$	$0.1\sin(0.1t)$	$0.5\sin(0.1t)$	$\sin(0.1t)$
$d_2(t)$	$0.2\sin(0.2t)$	$\sin(0.2t)$	$2\sin(0.2t)$
$\Delta f(x_1, x_2)$	$0.1\sin(0.2x_1 + 0.1x_2)$	$0.5\sin(0.2x_1 + 0.1x_2)$	$\sin(0.2x_1 + 0.1x_2)$

all the adaptive parameters. More specifically, it is shown in Fig. 7 that the purpose of suppressing unmodeled dynamics is achieved well by the dynamic auxiliary signal $r(t)$.

To show the robustness of the proposed FIAC method, a numerical simulation is carried out under three different cases, which is shown in Figs. 4 and 5. Three different cases correspond to three groups of different disturbances and model uncertain items, the specific values to be set are shown in the Table 2.

In order to present a fair comparison, here we take the same initial conditions and the controller parameters which are mentioned above. As illustrated in Figs. 4 and 5, although the tracking trajectories will fluctuate with the increase of disturbances and uncertainty, the overall tracking effects still meet the requirements, which shows that the proposed FIAC method has strong anti-disturbance ability and robustness.

5.0 Conclusions

In this paper, we have proposed a novel FIAC scheme for a class of uncertain nonlinear systems subject to full state constraints, unmodeled dynamics and disturbances. Different from most of the existing control shemes that consider unmodeled dynamics of system, this paper also solves the problem of coupling relationship between unmodeled dynamics and system states, and proposes a decoupling algorithm for coupling uncertainties using an auxiliary dynamic signal and BIAS-RBFNN. Among them, BIAS-RBFNN is an improved version of traditional RBFNN, which has stronger robustness and higher estimation accuracy. Moreover, the nonlinear error transformation technology adopted in this paper is simple and effective, which ensures the states of the system do not exceed the predefined time-varying asymmetric constraints and reduces the difficulty of controller design to a certain extent. By utilising mathematical inequality and a disturbance observer, both matched and mismatched disturbances are reasonably estimated and circumvented. Last but not least, through two groups of comparative simulations, it can be clearly seen that the proposed FIAC scheme in this work achieves satisfactory tracking performance without violating predefined full state constraints, and all closed-loop signals are bounded.

Acknowledgements. This work was supported by the National Natural Science Foundation of China under Grant (No. 62303378), the Foundation of China National Key Laboratory of Science and Technology on Test Physics & Numerical Mathematics under Grant (No. JP2022-800006000107-237, No. 08-YY-2023-R11), Science and Technology on Electromechanical Dynamic Control Laboratory of China under Grant (No. 6142601190210) and supported by the Foundation of Shanghai Astronautics Science and Technology Innovation under Grant (No. SAST2022-114).

References

[1] Liu, L., Li, X., Liu, Y. and Tong, S. Neural network based adaptive event trigger control for a class of electromagnetic suspension systems, *Control Eng. Pract.*, 2021, **106**, p 104675.

[2] Li, D., Chen, C., Liu, Y. and Tong, S. Neural network controller design for a class of nonlinear delayed systems with time-varying full-state constraints, *IEEE Trans. Neural Netw. Learn. Syst.*, 2019, **30**, (9), pp 2625–2636.

[3] Luo, X., Mu, D., Wang, Z., Ning, P. and Hua, C. Adaptive full-state constrained tracking control for mobile robotic system with unknown dead-zone input, *Neurocomputing*, 2023, **524**, pp 31–42.

[4] Wang, J., Yan, Y., Liu, Z., Chen, C., Zhang, C. and Chen, K. Finite-time consensus control for multi-agent systems with full-state constraints and actuator failures, *Neural Netw.*, 2023, **157**, pp 350–363.

https://doi.org/10.1017/aer.2024.120 Published online by Cambridge University Press

[5] Niu, B., Zhang, Y., Zhao, X., Wang, H. and Sun, W. Adaptive predefined-time bipartite consensus tracking control of constrained nonlinear MASs: An improved nonlinear mapping function method, *IEEE Trans. Cybern.*, 2023, **53**, (9), pp 6017–6026.
[6] Liu, L., Liu, Y., Chen, A., Tong, S. and Chen, C. Integral barrier Lyapunov function-based adaptive control for switched nonlinear systems, *Sci. China Inf. Sci.*, 2020, **63**, (3), pp 1–14.
[7] Liu, H., Zhao, S., He, W. and Lu, R. Adaptive finite-time tracking control of full state constrained nonlinear systems with dead-zone, *Automatica*, 2019, **100**, pp 99–107.
[8] Wang, C., Wu, Y., Wang, F. and Zhao, Y. TABLF-based adaptive control for uncertain nonlinear systems with time-varying asymmetric full-state constraints, *Int. J. Control*, 2021, **94**, (5), pp 1238–1246.
[9] Hua, C., Jiang, A. and Li, K. Adaptive neural network finite-time tracking quantized control for uncertain nonlinear systems with full-state constraints and applications to QUAVs, *Neurocomputing*, 2021, **440**, pp 264–274.
[10] Xia, D., Yue, X. and Wen, H. Output feedback tracking control for rigid body attitude via immersion and invariance angular velocity observers, *Int. J. Adapt. Control Signal Process.*, 2020, **34**, (12), pp 1812–1830.
[11] Wang, B., Yu, X., Mu, L. and Zhang, Y. Disturbance observer-based adaptive fault-tolerant control for a quadrotor helicopter subject to parametric uncertainties and external disturbances, *Mech. Syst. Sig. Process.*, 2019, **120**, pp 727–743.
[12] Cao, L., Xiao, B. and Golestani, M. Robust fixed-time attitude stabilization control of flexible spacecraft with actuator uncertainty, *Nonlinear Dyn.*, 2020, **100**, (3), pp 2505–2519.
[13] Liang, Z., Zhao, J., Dong, Z., Wang, Y. and Ding, Z. Torque vectoring and rear-wheel-steering control for vehicle's uncertain slips on soft and slope terrain using sliding mode algorithm, *IEEE Trans. Veh. Technol.*, 2020, **69**, (4), pp 3805–3815.
[14] Huang, J., Ri, S., Fukuda, T. and Wang, Y. A disturbance observer based sliding mode control for a class of underactuated robotic system with mismatched uncertainties, *IEEE Trans. Autom. Control*, 2018, **64**, (6), pp 2480–2487.
[15] Han, J., Kim, T., Oh, T. and Lee, S. Effective disturbance compensation method under control saturation in discrete-time sliding mode control, *IEEE Trans. Ind. Electron.*, 2019, **67**, (7), pp 5696–5707.
[16] Ran, M., Wang, Q., Dong, C. and Xie, L. Active disturbance rejection control for uncertain time-delay nonlinear systems, *Automatica*, 2020, **112**, (7), p 108692.
[17] Zhang, Y., Chen, Z., Zhang, X., Sun, Q. and Sun, M. A novel control scheme for quadrotor UAV based upon active disturbance rejection control, *Aerosp. Sci. Technol.*, 2018, **79**, pp 601–609.
[18] Ahi, B. and Haeri, M. Linear active disturbance rejection control from the practical aspects, *IEEE/ASME Trans. Mechatron.*, 2018, **23**, (6), pp 2909–2919.
[19] Sun, S., Ren, T. and Wei, X. Composite DOBC with fuzzy fault-tolerant control for stochastic systems with unknown nonlinear dynamics, *Int. J. Robust Nonlinear Control*, 2019, **29**, (18), pp 6605–6615.
[20] Ma, J., Xu, S., Cui, G., Chen, W. and Zhang, Z. Adaptive backstepping control for strict-feedback non-linear systems with input delay and disturbances, *IET Control Theory Appl.*, 2019, **13**, (4), pp 506–516.
[21] Ma, Z. and Ma, H. Adaptive fuzzy backstepping dynamic surface control of strict-feedback fractional-order uncertain nonlinear systems, *IEEE Trans. Fuzzy Syst.*, 2019, **28**, (1), pp 122–133.
[22] Bu, X., He, G. and Wei, D. A new prescribed performance control approach for uncertain nonlinear dynamic systems via back-stepping, *J. Frankl. Inst.*, 2018, **355**, (17), pp 8510–8536.
[23] Polycarpou, M. and Ioannou, P. A robust adaptive nonlinear control design, In *1993 American Control Conference*, 1993, pp 1365–1369.
[24] Wang, Z., Yuan, Y. and Yang, H. Adaptive fuzzy tracking control for strict-feedback markov jumping nonlinear systems with actuator failures and unmodeled dynamics, *IEEE Trans. Cybern.*, 2020, **50**, (1), pp 126–139.
[25] Lavretsky, E. and Wise, K. Robust adaptive control, *Robust Adap. Cont.*, 2013, pp 317–353.
[26] Liu, Y., Zeng, Q., Tong, S., Chen, C. and Liu, L. Adaptive neural network control for active suspension systems with time-varying vertical displacement and speed constraints, *IEEE Trans. Ind. Electron.*, 2019, **66**, (12), pp 9458–9466.
[27] Huang, X., Wen, C. and Song, Y. Adaptive neural control for uncertain constrained pure feedback systems with severe sensor faults: A complexity reduced approach, *Automatica*, 2023, **147**, pp 110701.
[28] Chen, P., Luan, X., Wang, Z., Zhang, T., Ge, Y and Liu, F. Adaptive neural optimal tracking control of stochastic nonstrict-feedback nonlinear systems with output constraints, *J. Frankl. Inst.*, 2023, **360**, (16), pp 12299–12338.
[29] Ni, J. and Shi, P. Adaptive neural network fixed-time leader-follower consensus for multiagent systems with constraints and disturbances, *IEEE Trans. Cybern.*, 2020, **51**, (4), pp 1835–1848.
[30] Liu, Q., Li, D., Ge, S., Ji, R., Ouyang, Z. and Tee, K. Adaptive bias RBF neural network control for a robotic manipulator, *Neurocomputing*, 2021, **447**, pp 213–223.
[31] Dai, S., Wang, C. and Luo, F. Identification and learning control of ocean surface ship using neural networks, *IEEE Trans. Ind. Inf.*, 2012, **8**, (4), pp 801–810.
[32] Cybenko, G. Approximation by superpositions of a sigmoidal function, *Math. Control Signals Syst.*, 1989, **2**, (4), pp 303–314.
[33] Jiang, Z. and Praly, L. Design of robust adaptive controllers for nonlinear systems with dynamic uncertainties, *Automatica*, 1998, **34**, (7), pp 825–840.

Cite this article: Yin Y., Ning X., Wang Z. and Li R. (2025). Full-state-constrained intelligent adaptive control for nonlinear systems with unmodeled dynamics and mismatched disturbances. *The Aeronautical Journal*, **129**, 1286–1302. https://doi.org/10.1017/aer.2024.120

https://doi.org/10.1017/aer.2024.120 Published online by Cambridge University Press